Eur. Phys. J. B **45**, 555–560 (2005)
DOI: 10.1140/epjb/e2005-00211-7

THE EUROPEAN PHYSICAL JOURNAL B

Scaling in convective evaporation and sidewall boundary layer

F. Perrier[a]

Laboratoire Hydrogéochimie et Études de sites, Commissariat à l'Énergie Atomique, B.P. 12, 91680 Bruyères-le-Châtel, France

Received 23 November 2004 / Received in final form 8 March 2005
Published online 13 July 2005 –

Abstract. Turbulent convection at aspect ratios from 0.06 to 2 is investigated in the laboratory with evaporation experiments from vertical cylinders having different diameters and liquid levels. With alcohol, only diffusive evaporation takes place. With water, for small diameters, evaporation proceeds by diffusion whereas convective evaporation develops when the diameter is increased. This onset can be effectively interpreted in terms of a viscous sidewall boundary layer, whose thickness δ varies with respect to the available height h according to $\delta/h = 3.4\ \mathrm{Ra}^{-0.28\pm0.01}$ versus Rayleigh number Ra. The Sherwood number Sh, analog of the Nusselt number, exhibits a power law variation $Sh = 0.6\ \mathrm{Ra}^{0.27\pm0.02}$ for Ra varying from 10^4 to 3×10^8. The scaling observed in this case of an open boundary is thus similar to the scaling measured in confined Rayleigh-Bénard convection.

PACS. 92.60.Jq Water in the atmosphere (humidity, clouds, evaporation, precipitation) – 47.27.-i Turbulent flows, convection, and heat transfer – 47.27.Sd Noise (turbulence generated) – 92.60.Ek Convection, turbulence, and diffusion

1 Introduction

Turbulent convection is a subject of active research in fluid dynamics, both because of the associated theoretical issues and because of its importance in engineering, geophysical, or environmental applications [1,2]. In particular, Rayleigh-Bénard (RB) laboratory experiments, where a closed box is heated from below and cooled from above, have been fruitful in giving access to fundamental results as well as to unexpected physics such as velocity fluctuations [3] or chaotic mean wind reversals [4]. However, while a unified framework for the scaling properties has been recently proposed [5], the values of the scaling parameters, the nature of the boundary layers, and the effect of the geometry of the cell, despite continued progress in the experiments [6–8], still need to be assessed in details. Furthermore, when considering situations such as, for example, the turbulent mixing of air in a chimney or the vertical access pit of an underground quarry [9], the applicability of the properties obtained from RB experiments is not necessarily straightforward. In any case, values of the aspect ratio, defined as the diameter over the height, smaller than 0.5 have been rarely explored [10]. In this paper, the results of evaporation experiments using vertical open cylinders are presented, with the aim of studying the links both to the RB system and to situations of practical interest.

[a] e-mail: perrier@ipgp.jussieu.fr
Also at Laboratoire de Géomagnétisme, Institut de Physique du Globe de Paris, 4, Place Jussieu, 75005 Paris, France

Evaporation experiments with water or other liquids have been fruitful tools to study the matter flux, analogous to thermal flux, in various isothermal or adiabatic forcing situations [11,12]. Such experiments offer interesting features: the liquid flux is determined with precision by weighing and sidewall conduction effects, known to be a significant problem in the interpretation of RB experiments [13,14], do not contribute in this case. In addition, they allow the investigation of an open system, where the interactions between plumes and mean wind must be different compared with the RB cell, especially at low aspect ratios. In this work, standard glass or polymer measuring beakers have been exposed in a ventilated laboratory room for long periods of time, by contrast with previous studies [11,12], thus averaging humidity and temperature variations. In addition, results are presented after normalization to the simultaneously measured diffusive flux, thus removing part of the uncertainties associated with the varying humidity conditions or the knowledge of the boundary conditions.

Consider a tube of diameter d containing a liquid whose level is defined by the distance h measured from the upper rim, exposed to air in a stirred room characterized by a homogeneous vapor partial pressure p_V in the air. The flux F, defined as the evaporative liquid mass loss per unit time per unit area, includes a convective contribution and a purely diffusive contribution F_D. The latter is:

$$F_D = D\frac{c_s}{h}\left(1 - RH\right), \qquad (1)$$

Table 1. Summary of the parameters of the beakers and the tube. The exponents correspond to power-law fits of Sh versus Ra (Fig. 6). P stands for Polypropylene, PMP for Polymethylpentene, Pg for Plexyglass and G for Glass.

Type	Number	Nature	Diameter (mm)	Exponent
Test tubes	15	G	8.3	
10 mL	6	P	11.9	
25 mL	5	P and G	16.3	
50 mL	4	P	23.1	
100 mL	6	P and G	27.2	
250 mL	4	G	37.3	0.34
500 mL	5	P and G	49.7	0.32
1000 mL	6	G	59.5	0.31
2000 mL	3	G	79.2	0.28
4000 mL	3	PMP	102.1	0.24
Long Tube	1	Pg	80.3	0.24

where D is the diffusion coefficient of vapor in air (2.1×10^{-5} m^2 s^{-1} for water vapor), c_s is the saturated vapor concentration (17.3 g m^{-3} at 20 °C for water) and $RH = p_v/p_s$, with p_v and p_s being respectively the vapor partial pressure and the saturated vapor pressure (2337 Pa at 20 °C) in air at saturation. The evaporative flux F_C in the presence of convection is written $F_C = F_D$Sh, where Sh is the Sherwood number [11], analogous to the Nusselt number of thermal convection [1]. The convection is controlled by a forcing parameter, the Rayleigh number Ra, defined as [11]:

$$\mathrm{Ra} = \frac{g\,(\rho - \rho_s)\,h^3}{\nu D}, \qquad (2)$$

where ρ and ρ_s are respectively the density of air in the room and of air saturated with water with respect to dry air, g the acceleration of gravity, and ν is the kinematic viscosity of air (15.9×10^{-6} m^2 s^{-1} at 20 °C).

2 Evaporation experiments

More than 40 cylindrical measuring beakers of varying volumes and diameters (Tab. 1), and for each type, of varying liquid levels, were exposed simultaneously. Cylinders of varying nature (glass, polypropylene and polymethylpentene) were used (Tab. 1) and, when available, compared for the same cylinder volume. One additional experiment was performed with ethanol using 15 glass test tubes and a subset of polypropylene beakers. In addition, in order to expand the Ra range, one vertical plexyglass tube of length 130 cm was used with water.

The ventilated room is characterized by an average temperature of 22 °C, stable within 1 °C in winter but reaching 24 °C in summer, with a diurnal amplitude reaching 2 °C peak to peak. The relative humidity in the room RH varies between 20 and 50%, mostly on a daily cycle with 10% amplitude peak to peak. Ventilation of the room is maintained by a mechanical air circulation circuit with vents located in one side of the room, 20 cm above floor level. The cylinders are placed on tables, about 6 m from the vents. During the experiment, some cylinders were shifted to another table 12 m away from the vents; no systematic effect resulted from this change.

Two balances were used for weighing the cylinders: one Sartorius^{TM} BP110 model with maximum range 110 g and precision 0.001 g and one Mettler^{TM} Toledo PG50002-S model with maximum range 5100 g and precision varying from 0.01 to 0.1 g. Both balances were recalibrated every six months with reference weights. In addition, the stability of the balances was checked regularly with reference weights, empty reference cylinders, and intercomparison experiments were performed to check the two balances in their overlapping range. The time lapse between two measurements varied from one to six weeks and the experiment lasted from July 2002 to March 2004, except for the 4000 mL measuring beakers and the long tube, which were introduced in March 2003 only. The mass difference between two measurements was typically 40 g for 2000 mL cylinders and 250 mg for 10 mL cylinders with water.

Most measurements were performed with tap water. Using degassed de-ionized water changed the evaporation flux by less than 2%. Some experiments were performed with ethanol (95% grade). The water level h (distance from meniscus to rim) is obtained from the mass m of liquid and an experimental determination for each cylinder of the relationship m-h.

3 Results

The measured flux is shown in Figure 1 as a function of h for water evaporated from the 10 mL measuring cylinders, and for ethanol evaporated from the test tubes. Data points for ethanol have been obtained over three days, whereas the data points for water correspond to the whole duration of the experiment (1.5 year). For water, large time variability (about a factor of 2) is observed, corresponding to situations with and without heating in the laboratory. At a given time, however, data points obtained for different values of h lie on the same line, with a slope -1 in this graph, which corresponds to the $1/h$ factor expected from pure diffusion in equation (1). This indicates that the evaporative flux for the 10 mL measuring cylinders is dominated by a diffusion process, and that the boundary condition is effectively located near the upper rim of the cylinder.

In the case of ethanol, the $1/h$ variation is observed over most of the h range. A slight deviation can nevertheless be observed for h smaller than 2 cm, which can be accounted for by a $1/(h - 0.4$ cm) behavior (Fig. 1). This may reflect the meniscus curvature or the thickness of a vapor saturated boundary layer of air located above the liquid surface. In the following, although a minor change, h is corrected for this effect by subtracting 0.4 cm. The measured value of the quantity $F \times h$ is 0.25 ± 0.03 g cm^{-1} day^{-1} for water. The theoretical value expected from equation (1) is 0.204 ± 0.047 g cm^{-1} day^{-1} for a mean relative humidity of 35 ± 15% in the room. The observed value is compatible with the calculation but is slightly larger, which may indicate the need of introducing

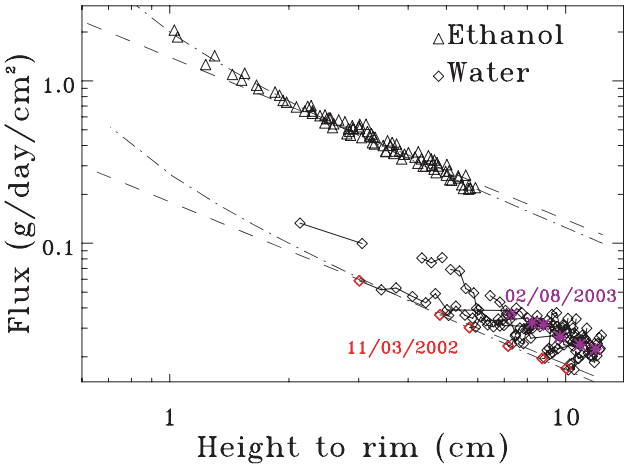

Fig. 1. Evaporation flux as a function of water level h (height to rim) for 10 mL polypropylene cylinders with water and 8.3 mm diameter glass tubes with ethanol. Dotted lines correspond to the $1/h$ slope. Dashed lines correspond to $1/(h-0.4)$. Attached data points correspond to the same beaker at different times. Two sets of simultaneous measurements with water are emphasized: red diamonds (November 3, 2002) and purple diamonds (February 8, 2003).

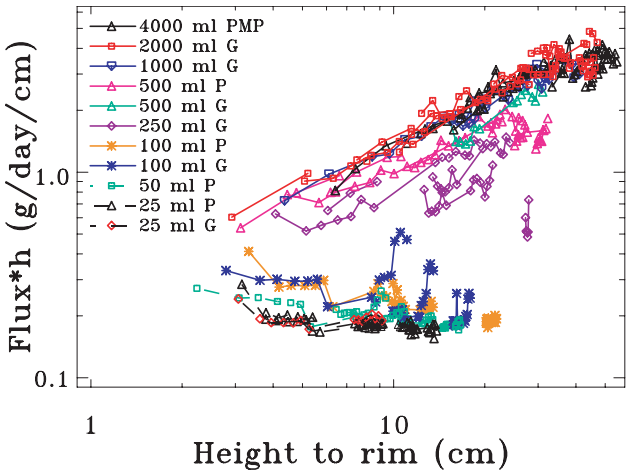

Fig. 2. Evaporative flux multiplied by water level h as a function of h for three 2000 mL glass cylinders (Tab. 1). Attached data points correspond to the same cylinder at different times.

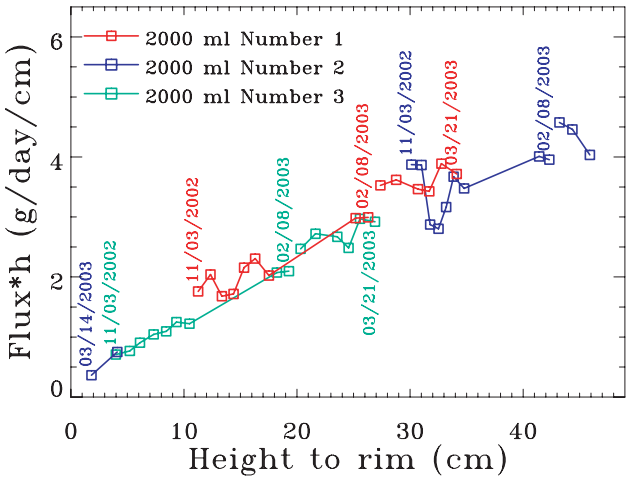

Fig. 3. Evaporative flux multiplied by water level h as a function of h for three 2000 mL glass cylinders (Tab. 1). Attached data points correspond to the same cylinder at different times.

a turbulent diffusion coefficient or the presence of pumping associated to the daily humidity cycle in the room.

A different behavior is observed when the diameter is increased. The product $F \times h$ is shown as a function of h in Figure 2 for all measuring beakers. In this figure, in order to reduce most of the dispersion due to the time variability of the evaporative forcing, the data have been normalized to the value observed in the 10 mL measuring cylinders, taken as reference. For 25 mL, 50 mL and 100 mL measuring beakers, $F \times h$ is stable with h or is slightly decreasing as a function of h, whereas $F \times h$ is increasing steeply for the 1000 mL, 2000 mL and 4000 mL beakers. An intermediate behavior is observed for 250 mL and 500 mL cylinders, which have also a larger dispersion.

The data of the independent beakers of the same type at a given time, and the data of one given beaker followed over time, tend to fall on the same average curve versus h. This is illustrated in Figure 3 for three 2000 mL beakers. The consistency of the results is remarkable, which also indicates that aging effects, due for example to dust deposition, do not affect significantly the evaporative flux in these experiments. A contribution of aging also could not be identified when water was renewed.

In Figure 2, the results are presented separately for glass and polypropylene beakers when both types were available at a given diameter (see Tab. 1). Non-isothermal conditions at the evaporating surface would be expected to give different effects with glass and polypropylene. No systematic difference however is observed in the case of the 25 mL and 100 mL cylinders. For 500 mL cylinders, a larger flux is noticed for h larger than 20 cm. With this possible exception, non-isothermal effects can be considered negligible in most of our data sample. This is probably due to the relatively large amount of water in the cylinders for most data points.

The variation of the product $F \times h$ as a function of d is shown in Figure 4 for fixed values of h (4 cm, 10 cm and 30 cm). To obtain the data points of Figure 4, for each specified value of h, the data points for fixed d as a function of h (Fig. 2) have been interpolated using power-law fits. A clear threshold behavior emerges as a function of d in Figure 4. For small values of d, the flux is small, compatible with diffusion only. When the diameter is increased, the flux increases suddenly by a factor of 10, indicating a brutal onset of convective evaporation.

4 Interpretation

The interpretation of the onset of convective flux when the diameter is increased may not be straightforward. In some

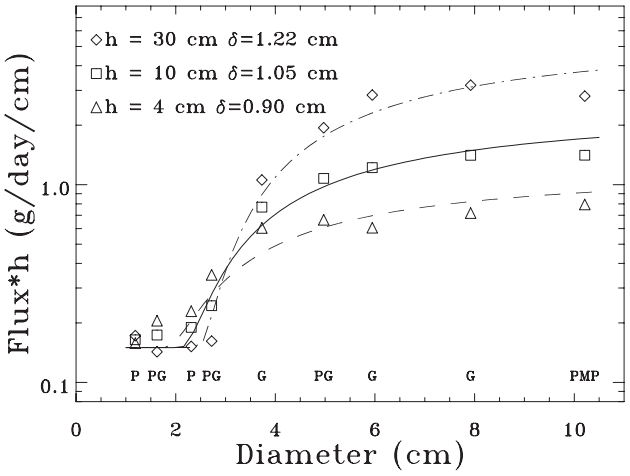

Fig. 4. Evaporative flux multiplied by water level h as a function of the diameter for fixed values of h. The lines correspond to geometrical restriction of convection due to the sidewall boundary layer of thickness δ, as described by equation (3). P stands for Polypropylene, PMP for Polymethylpentene, G for Glass.

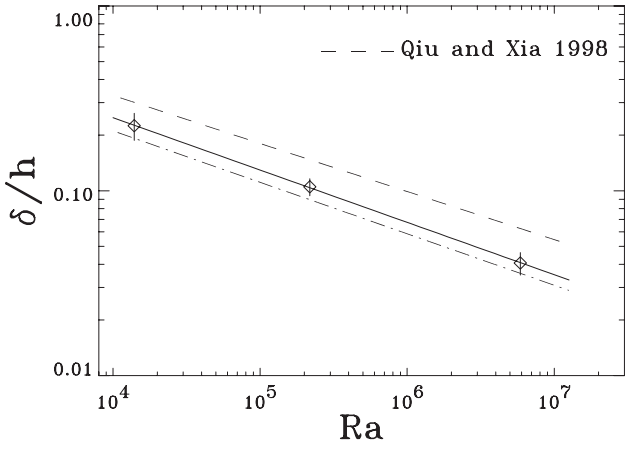

Fig. 5. Scaled sidewall boundary layer thickness δ/h versus Rayleigh number Ra. The data points correspond to the determination of Figure 4. Error bars correspond to the difference between the preferred values of thickness δ and the values obtained from a three-parameter fit of equation (3) to the data. The full line corresponds to the power-law fit 3.4 $\mathrm{Ra}^{-0.28}$ from the data. The dotted line corresponds to the fitted values of the thickness. The dashed line corresponds to the power-law fit 3.6 $\mathrm{Ra}^{-0.26}$ given by Qiu and Xia [7].

experiments [12], convection was observed to be blocked by a supposed open thermosyphon mechanism in particular circumstances. It must be pointed out, however, that such situation is not likely to occur in the present experiment, where measurements are averaged over long periods of time and where several daily cycles are likely to prevent the stabilization of blocked configurations. Rather, one could propose an effect due to a purely geometrical restriction of the convection cells.

Indeed, the convection processes could be simply restricted by the presence of a viscous boundary layer along the wall of the vertical cylinder. Thus, for a thickness δ of the boundary layer, a cylinder of diameter $d - 2\delta$ only is available for convective transport of liquid vapor. Because of this geometrical restriction, the measured flux F can be written:

$$F = F_C \left(1 - \frac{2\delta}{d}\right)^2 + F_D \left[1 - \left(1 - \frac{2\delta}{d}\right)^2\right]. \quad (3)$$

Assuming that both the convective and diffusive contributions do not depend on the diameter, the variation of F with diameter is due to the geometrical restriction only. The flux predicted by equation (3) as a function of d is also shown in Figure 4 (curves). For each of the selected value of h, the predicted curves for the indicated values of δ provide a satisfactory description of the observed variation of F with diameter. When the sidewall boundary layer is introduced in this manner, therefore, it does not appear necessary to invoke a variation of the convection flux F_C with diameter, at least for the range of aspect ratios (0.06 to 2) considered here. While this interpretation cannot be considered unique, it is supported by the data of Figure 4. Equation (3) might actually be an efficient manner to take into account complicated effects associated with restriction of particular convective modes. Thus, this sidewall boundary layer may be more properly referred to as effective or apparent.

The obtained values of the thickness δ are: 0.90 ± 0.15, 1.05 ± 0.11, and 1.22 ± 0.17 cm for $h = 4$, 10, and 30 cm, respectively. These values are obtained by trial and error. A three parameter fit of equation (3) to the data gives $\delta = 0.72$, 0.90 and 1.05 cm respectively. But this fit is rather poorly constrained and the trial and error values are preferred. The difference with the fit values provides our estimate of the error bar on δ. Note that these values suggest a significant variation of δ as a function of h, a fact which is actually visible on the behavior of the data points as a function of d in Figure 4. The scaled thickness of the boundary layer, defined as the ratio δ/h, is shown in Figure 5 as a function of Ra, calculated using equation (2). A power-law fit to these three data points gives $\delta/h = 3.4\ \mathrm{Ra}^{-0.28\pm0.01}$, which is in good agreement with the power-law fit $\delta/h = 3.6\ \mathrm{Ra}^{-0.26\pm0.03}$ obtained in RB convection experiments with water [7].

Using the obtained expression of δ/h as a function of Ra, the observed evaporation flux F can be corrected for the diameter effect, represented by equation (3), and the non-diffusive flux F_C can be inferred. The Sherwood number is then calculated as a function of Ra using $Sh = F_C/F_D$. The diffusive flux F_D is given by the value measured simultaneously with the 10 mL beakers, shown previously to be dominated by diffusive evaporation (Fig. 1). The results are shown in Figure 6 as a function of Ra for the 2000 mL beakers and the tube. In this figure, the data points from single mass measurements are averaged in intervals of Ra. Note that the data obtained with the long plexyglass tube are consistent with the data from the 2000 mL glass beakers, and allow to expand the Ra range by almost two orders of magnitude up to 3×10^8. Using the data

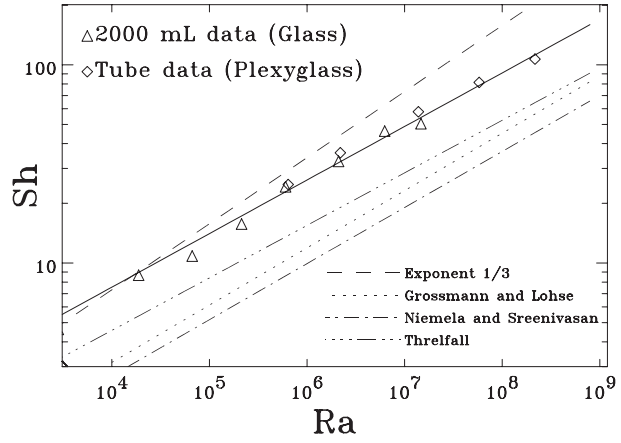

Fig. 6. Sherwood number Sh versus Rayleigh number Ra. Symbols correspond to the averaged data from the 2000 mL glass beakers (triangles) and the plexyglass tube (diamonds). Statistical error bars resulting from the averaging are smaller than the size of the symbols. The full line corresponds to the power-law fit 0.60 $\mathrm{Ra}^{0.27\pm0.02}$ obtained using data from the 2000 mL beakers and the tube. The dashed line corresponds to $\mathrm{Ra}^{1/3}$. The dotted line corresponds to 0.22 $\mathrm{Ra}^{0.289}$ [5], the dash-dot line to 0.20 $\mathrm{Ra}^{0.283}$ obtained by fitting the data from [6] for Ra smaller than 10^9; the dash-triple dot line corresponds to 0.398 $\mathrm{Ra}^{0.265}$ for aspect ratio 0.14 by Threlfall [10].

from the 2000 mL beakers and the tube, a power-law fit $Sh = 0.60\mathrm{Ra}^{0.27\pm0.02}$ is obtained. Similar values of the exponent are also obtained from the other beakers (Tab. 1). In contrast, the evaporation experiment performed using the beakers and ethanol yields $Sh = 1.14 \pm 0.07$. This result can be understood. As the molecular mass of ethanol is 46.1 g, indeed, the density of ethanol vapor saturated air is larger than the density of the room air, and therefore buoyant convective transport cannot take place in this case. It may be pointed out that the result obtained with alcohol is non-trivial. It supports the hypothesis that the boundary conditions operating in the room for the small 10 mL beakers are also valid for the large diameter 2000 mL cylinders, whose rim is located 35 cm higher than the rim of the 10 mL beakers. The room therefore can be considered, at least on average, as a well-mixed homogeneous boundary for all the cylinders. This condition is not necessarily satisfied when the evaporating tubes are placed in a box with a gradual variation of humidity between the rim of the cylinders and some constrained surface in the box [12].

5 Summary and discussion

Evaporation experiments for varying diameters and liquid levels reported in this paper are characterized by sampling over long period of times. In addition, the measured fluxes are normalized to the simultaneously measured diffusive flux with 10 mL cylinders, and some uncertainties are cancelled out in this ratio. The detailed study of the diffusive flux versus liquid level and the comparison, for larger cylinders, between water and alcohol evaporation losses, provide some access to the otherwise poorly known boundary conditions.

The observed scaling of Sh versus Ra is compared in Figure 6 with the scaling $Nu = 0.22\ \mathrm{Ra}^{0.289}$ obtained from RB convection [5]. Recent results [6], fitted for Ra smaller than 10^9, give $Nu = 0.20\ \mathrm{Ra}^{0.283}$. Note that a smaller exponent 0.265 is documented for aspect ratio $d/h = 0.14$ (Threlfal in [10]). Hence, both the behavior of the viscous boundary layer and the exponent of the convective flux observed in the open evaporation experiments reported here are in astonishing agreement with the results obtained from closed RB cells. This suggests that, at least in the turbulent regimes, convection adopts universal scaling exponents, independent of the exact nature of the physical system, in particular the source of buoyancy. The details of the physical system seem to be contained in the cofactor. The agreement between the scaling of the boundary layer obtained in this experiment and the scaling obtained from RB experiment [7] is particularly significant because the method of inference is extremely different in the latter case, which was based a scanning of temperature as a function of the distance to the wall.

This experiment also suggests that, in the covered range 0.06 to 2 of the aspect ratio d/h, in a first approximation, no additional aspect-ratio-dependent scaling exponent needs to be introduced. Although aspect ratio is known to affect the convection cells [1,2,10] at least for d/h varying between 0.5 and 2, such effects may appear only for confined convection. For open convection, for example at work in evaporating cylinders or chimneys, the geometry of the turbulent cells may be constrained by falling and rising plumes, thus perhaps removing all geometrical constraints except the sidewall boundary layer.

The fact that the value of the scaling exponent obtained in this experiment remains significantly smaller than 1/3 suggests that, since evaporation experiments are free of wall contributions, the value close to 2/7 observed in RB cells [1] could be significant and may not need to be explained by a modification of 1/3 due to a wall effect [12,13]. This conclusion however must remain tentative, given the current insufficient accuracy on the exponent from the evaporation experiments; the wall effects still deserve to be investigated in details.

Several limitations of the evaporation experiments presented here need to be pointed out. The role of the temperature changes at the liquid surface due to the phase changes could affect the observed flux in some cases. The level of accuracy obtained so far for the data points of Sh versus Ra certainly does not compare with the outstanding precision achieved in RB cells.

Despite their imperfections, evaporation experiments could be worth improving. Five orders of magnitude in Ra have been explored in this experiment and this range can be expanded further in the hard turbulence regime by using longer tubes. More precise experiments, performed for example in a large climatic chamber with well defined and stable conditions, may be able to better constrain the sidewall boundary layers. Finally, these experiments

suggest that the values of the exponents derived from RB cells can potentially be applied to practical situations, including open systems. This universality needs to be tested further in well controlled laboratory or large-scale natural systems.

The author thanks Jean-Louis Le Mouël, Jean-Paul Poirier and Patrick Richon for suggestions and Eric Pili for support. Two anonymous reviewers are thanked for inspiring comments and for raising important points in the original manuscript. This work is IPGP contribution number 2063.

References

1. B. Castaing, G. Gunaratne, F. Heslot, L. Kadanoff, A. Libchaber, S. Thomae, X.-Z. Wu, S. Zaleski, G. Zanetti, J. Fluid Mech. **204**, 1 (1989)
2. R. Verzicco, R. Camussi, J. Fluid Mech. **477**, 201 (2003)
3. X.-L. Qiu, X.-D. Shang, P. Tong, K.-Q. Xia, Phys. Fluids **16**, 412 (2004)
4. K.R. Sreenivasan, A. Bershadskii, J.J. Niemela, Phys. Rev. E **65**, 056306 (2002)
5. S. Grossmann, D. Lohse, J. Fluid Mech. **407**, 27 (2000)
6. J.J. Niemela, K.R. Sreenivasan, J. Fluid Mech. **481**, 355 (2003)
7. X.-L. Qiu, K.-Q. Xia, Phys. Rev. E **58**, 486 (1998)
8. S. Lam, X.-D. Shang, S.-Q. Zhou, K.-Q. Xia, Phys. Rev. E **65**, 066306 (2002)
9. F. Perrier, P. Morat, J.-L. Le Mouël, Phys. Rev. Lett. **89**, 134501 (2002)
10. X.-Z. Wu, A. Libchaber, Phys. Rev. A **45**, 842 (1992)
11. E.M. Sparrow, G.A. Nunez, Int. J. Heat Mass Transfer **31**, 1345 (1988)
12. G.D. McBain, H. Suehrcke, J.A. Harris, Int. J. Heat Mass Transfer **43**, 2117 (2000)
13. P.-E. Roche, B. Castaing, B. Chabaud, B. Hébral, J. Sommeria, Eur. Phys. J. B **24**, 405 (2001)
14. R. Verzicco, J. Fluid Mech. **473**, 201 (2002)